Supporting Information

Cobalt MOF-Derived Co/CoO/C Composites for Efficient Peroxymonosulfate Activation and Oxytetracycline Degradation

Jia-Hong She,[†] *Mi-Zhen Sun,*[‡] *Shu-Ran Zhang,**[*,†] *Guang-Juan Xu,*[†] *Yan-Hong Xu*,[*,†] *Wei Xie,*[†] *Xiao-Li Hu,*[§] *Zhong-Min Su,*[*,§]

[†]Key Laboratory of Preparation and Applications of Environmental Friendly Materials (Jilin Normal University), Ministry of Education, Changchun, 130103, China

[‡]Shandong Engineering Research Center of Green and High-value Marine Fine Chemicals, Weifang University of Science and Technology, Shouguang, Shandong 262700, China

[§]School of Chemistry and Environmental Engineering, Changchun University of Science and Technology, Changchun, 130022, China

Email: zhangshuran2016@jlnu.edu.cn; xuyh198@163.com; zmsu@nenu.edu.cn

Table of contents

1. Tables

2. Figs

Materials and Methods. Cobalt nitrate hexahydrate, Peroxymonosulfate ($Co(NO_3)_2 \cdot 6H_2O$, PMS, Shanghai Aladdin Reagent Co., LTD), 1,4-naphthalenedicarboxylic (1,4-NDA, Adamas-beta), 1,4-bis(imidazol-1-ylmethyl)benzene (BIMB, Jilin Chinese Academy of Sciences-Yanshen Technology Co., LTD), N,N-dimethylacetamide (DMA, Tianjin Fuyu Fine Chemical Co., LTD), Deionized water (H_2O), oxytetracycline (OTC, Sinopharm Chemical Reagent Co., LTD), Methanol (MeOH, Tianjin Fuyu Fine Chemical Co., LTD), Tert-butanol (TBA, RON), P-benzoquinone, L-histidine (P-BQ, L-His, Shanghai Maclin Biochemical Technology Co., LTD), Sodium hydroxide (NaOH, Fuchen Tianjin Reagent Co., LTD), Hydrochloric acid (HCl, Beijing Chemical Plant), Sodium chloride (NaCl, Tianjin DingshengXin Chemical Co., LTD), Crystalline sodium carbonate ($NaCO_3 \cdot 10H_2O$, Shenyang Reagent Factory), Sodium dihydrogen phosphate (NaH_2PO_4, Tianjin Damao Chemical Reagent Factory), Sodium bicarbonate ($NaHCO_3$, Kaiyuan Chemical Reagent Factory). All reagents were used directly as supplied without further purification.

X-ray single crystal diffraction data of JLNU-15 were collected using Bruker Smart Apex III Diffractometer equipped with a Mo target (Kα, λ = 0.71073 Å) at room temperature. The structure of JLNU-15 was analyzed by the direct method and refined by the full matrix least-squares refinements utilizing the SHELXTL-97 program package. All non-hydrogen atoms underwent anisotropic refinement. The crystal structure information of JLNU-15 was shown in Table S1. The CIF file for JLNU-15 has been deposited in the Cambridge Crystallography Data Centre (CCDC), and CCDC number is 2413374. Elemental microanalyses (C, H, and N) were performed on a EuroEA-3000 elemental analyzer. Powder X-ray diffraction (PXRD) was performed on a Rigaku model RINT Ultima III diffractometer in the range of 3-60° at 293 K by depositing powder on glass substrate. Thermogravimetric analysis (TGA) was performed on a Q5000IR analyzer (TA Instruments) with an automated vertical overhead thermobalance heated from 50 to 1000 °C at a ramp rate of 5 °C min^{-1} under nitrogen atmosphere. Fourier transform Infrared (FT-IR) spectra were recorded in the range 4000–400 cm^{-1} on a Perkin-elmer FT-IR-frontier infrared spectrometer using KBr pellets.

Analysis method of degradation experiment. First, 20.0 mg of the antibiotic oxytetracycline was weighed with an analytical balance. Transfer to 50 mL beaker and add appropriate amount of deionized water to dissolve, then transfer to 100 mL volumetric bottle and prepare 200 mg/L oxytetracycline solution. In the process of degradation, the initial concentration of 200 mg/L of the pollutant is diluted to 20 mg/L. Before the degradation experiment began, Co/CoO/C-800 was added to establish an adsorption-desorption equilibrium under dark conditions. PMS was then added to trigger the degradation reaction. The whole reaction is stirred on a magnetic stirrer at a speed of 400 r/min. In the subsequent process, a small part of the reaction liquid is absorbed into the centrifuge tube, and the clear part is absorbed into the colorimetric dish, and the UV-visible spectrophotometer is used to determine the change of absorbance at a specific wavelength. According to the measured data, the degradation curve was drawn to analyze the catalytic degradation performance of the catalyst in the system.

The absorption wavelength of oxytetracycline is 355 nm. The absorbance of the degradation UV-vis absorption spectrum is measured in the range of 200-600 nm. Equation (1) was used to calculate the degradation efficiency of tetracycline, and the pseudo-first-order kinetic model as shown in equation (2) was used to study the degradation process of oxytetracycline:

$$\eta\ (\%) = (C_0 - C)/C_0 \times 100\% \qquad (1)$$

$$-\ln(C/C_0) = kt \qquad (2)$$

Here, C_0 is the initial concentration of oxytetracycline (mg/L), and C is the concentration of pollutants at time t (mg/L). k is the reaction rate constant in min^{-1}.

Table S1. Crystal Data and Structure Refinements for JLNU-15.

Identification code	JLNU-15

Empirical formula	$C_{52}H_{40}Co_2N_8O_8$
Formula weight	1020.79
Temperature (K)	294.96
Crystal system	triclinic
Space group	P-1
a (Å)	10.5121(6)
b (Å)	11.5698(5)
c (Å)	19.0923(10)
α (°)	96.406(2)
β (°)	93.983(3)
γ (°)	101.347(2)
Volume (Å^3)	2252.5(2)
Z	2
ρ_{calc} (g/cm^3)	1.505
μ (mm^{-1})	0.803
F (000)	1050.0
Radiation	MoKα (λ = 0.71073)
2θ range for data collection (°)	5.216 to 50.15
Index ranges	-12≤h≤12, -13≤k≤13, -22≤l≤22
Reflections collected	34323
Independent reflections	7910
Data/restraints/parameters	7910/0/631
Goodness-of-fit on F^2	1.053
Final R indexes [I>=2σ (I)]	R_1 = 0.0528, wR_2 = 0.1235
Final R indexes [all data]	R_1 = 0.0830, wR_2 = 0.1372

$^aR_1 = \Sigma||F_o|- |F_c||/\Sigma|F_o|$. $^bwR_2 = |\Sigma w(|F_o|^2-|F_c|^2)|/\Sigma|w(F_o^2)^2|^{1/2}$

Table S2. Bond angles (°) for JLNU-15.

Atom	Atom	Atom	Angle/˚	Atom	Atom	Atom	Angle/˚
O2	Co1	O6[1]	145.24(17)	C9	C7	C20	118.0(5)
O2	Co1	O7[1]	96.50(15)	C1	C8	C9	120.8(5)
O2	Co1	N3	111.91(17)	C7	C9	C8	120.6(5)
O2	Co1	N4[2]	95.57(16)	C11	C10	C27	120.4(5)
O6[1]	Co1	O7[1]	58.89(15)	C16	C10	C11	120.4(5)
N3	Co1	O6[1]	90.61(16)	C16	C10	C27	119.0(5)

N3	Co1	O7[1]	149.41(16)	C5	C11	C10	118.5(4)
N3	Co1	N4[2]	99.07(17)	C5	C11	C28	119.5(5)
N4[2]	Co1	O6[1]	107.03(17)	C28	C11	C10	121.9(5)
N4[2]	Co1	O7[1]	88.83(17)	C23	C12	C3	120.4(5)
O1	Co2	O5	137.57(17)	O2	C13	C6	117.1(4)
O1	Co2	N1[2]	95.55(16)	O4	C13	O2	121.4(5)
O1	Co2	N2	114.93(16)	O4	C13	C6	121.4(5)
O5	Co2	N1[2]	108.30(18)	N2	C14	N8	110.0(5)
O5	Co2	N2	95.03(17)	N7	C15	N4	111.4(5)
N2	Co2	N1[2]	100.50(17)	C10	C16	C21	120.6(5)
C2	O1	Co2	103.4(3)	N3	C17	N5	110.8(5)
C13	O2	Co1	105.3(3)	C38	C18	N2	109.5(5)
C27	O5	Co2	104.7(4)	C30	C19	C5	120.3(5)
C20	O6	Co1[3]	95.1(3)	O6	C20	O7	120.1(5)
C26	N1	Co2[4]	122.6(3)	O6	C20	C7	119.1(5)
C26	N1	C37	105.1(4)	O7	C20	C7	120.8(5)
C37	N1	Co2[4]	132.1(4)	C6	C21	C16	120.9(5)
C14	N2	Co2	123.4(4)	C25	C22	C23	120.3(5)
C14	N2	C18	105.9(4)	C12	C23	C22	120.9(5)
C18	N2	Co2	128.7(3)	C39	C24	C47	120.3(5)
C20	O7	Co1[3]	85.9(3)	C42	C24	C39	120.8(6)
C17	N3	Co1	123.1(3)	C42	C24	C47	118.8(6)
C17	N3	C32	106.2(4)	C22	C25	C4	120.8(5)
C32	N3	Co1	128.5(4)	N1	C26	N6	111.6(5)
C15	N4	Co1[4]	124.8(4)	O5	C27	C10	115.8(5)
C15	N4	C50	105.2(5)	O8	C27	O5	122.8(5)
C50	N4	Co1[4]	129.9(4)	O8	C27	C10	121.4(5)
C17	N5	C41	107.9(4)	C34	C28	C11	120.5(5)

C17	N5	C47	125.9(5)	C44	C29	C40	121.6(5)
C41	N5	C47	125.8(5)	C44	C29	C48	119.0(5)
C26	N6	C31	124.2(5)	C48	C29	C40	119.2(5)
C26	N6	C36	106.4(5)	C19	C30	C34	120.9(5)
C36	N6	C31	129.4(5)	N6	C31	C33	109.9(5)
C15	N7	C51	125.6(5)	C41	C32	N3	109.0(5)
C15	N7	C52	108.4(5)	C35	C33	C31	120.7(5)
C52	N7	C51	125.9(6)	C35	C33	C49	118.6(5)
C14	N8	C38	108.8(5)	C49	C33	C31	120.6(5)
C14	N8	C40	126.5(5)	C28	C34	C30	120.2(5)
C38	N8	C40	124.7(5)	C33	C35	C44	120.4(5)
C3	C1	C2	122.2(4)	N6	C36	C37	107.7(5)
C8	C1	C2	118.0(4)	C36	C37	N1	109.2(5)
C8	C1	C3	119.7(4)	C18	C38	N8	105.7(5)
O1	C2	C1	116.9(4)	C24	C39	C45	120.0(5)
O3	C2	O1	121.8(4)	N8	C40	C29	111.3(5)
O3	C2	C1	121.1(4)	C32	C41	N5	106.0(5)
C1	C3	C4	119.2(4)	C24	C42	C43	119.4(6)
C1	C3	C12	121.7(4)	C46	C43	C42	120.6(6)
C4	C3	C12	118.9(4)	C29	C44	C35	120.5(5)
C3	C4	C7	118.7(4)	C46	C45	C39	118.6(6)
C3	C4	C25	118.6(5)	C43	C46	C45	120.6(6)
C7	C4	C25	122.5(4)	C43	C46	C51	120.1(6)
C6	C5	C19	121.7(4)	C45	C46	C51	119.3(7)
C11	C5	C6	119.8(4)	N5	C47	C24	113.1(5)
C11	C5	C19	118.4(5)	C49	C48	C29	120.4(6)
C5	C6	C13	122.1(4)	C48	C49	C33	121.0(6)
C21	C6	C5	119.4(4)	N4	C50	C52	110.4(6)

C21	C6	C13	118.3(4)	N7	C51	C46	109.8(5)
C4	C7	C20	121.6(4)	N7	C52	C50	104.5(6)
C9	C7	C4	120.3(4)				

[1]+X,+Y,-1+Z;[2]1+X,1+Y,+Z;[3]+X,+Y,1+Z;[4]-1+X,-1+Y,+Z

Table S3. Bbond lengths (Å) for JLNU-15.

Bond Lengths (Å)					
Atom	**Atom**	**Length/Å**	**Atom**	**Atom**	**Length/Å**
Co1	O2	1.984(3)	C4	C7	1.427(7)
Co1	O6[1]	2.099(4)	C4	C25	1.429(7)
Co1	O7[1]	2.289(4)	C5	C6	1.433(7)
Co1	N3	2.047(4)	C5	C11	1.421(7)
Co1	N4[2]	2.081(4)	C5	C19	1.437(7)
Co2	O1	1.983(3)	C6	C13	1.496(7)
Co2	O5	1.996(4)	C6	C21	1.371(7)
Co2	N1[2]	2.084(4)	C7	C9	1.356(7)
Co2	N2	2.046(4)	C7	C20	1.512(7)
O1	C2	1.277(6)	C8	C9	1.421(7)
O2	C13	1.268(6)	C10	C11	1.436(7)
O3	C2	1.227(6)	C10	C16	1.363(8)
O4	C13	1.240(6)	C10	C27	1.525(7)
O5	C27	1.259(7)	C11	C28	1.424(7)
O6	C20	1.242(6)	C12	C23	1.378(7)
N1	C26	1.331(7)	C16	C21	1.422(7)
N1	C37	1.368(7)	C18	C38	1.358(8)
N2	C14	1.328(7)	C19	C30	1.375(8)
N2	C18	1.395(7)	C22	C23	1.400(8)
O7	C20	1.255(7)	C22	C25	1.382(8)

O8	C27	1.226(7)	C24	C39	1.388(9)
N3	C17	1.328(6)	C24	C42	1.380(8)
N3	C32	1.377(7)	C24	C47	1.529(8)
N4	C15	1.329(7)	C28	C34	1.376(8)
N4	C50	1.353(8)	C29	C40	1.514(8)
N5	C17	1.338(7)	C29	C44	1.387(8)
N5	C41	1.373(7)	C29	C48	1.401(8)
N5	C47	1.466(7)	C30	C34	1.410(8)
N6	C26	1.349(7)	C31	C33	1.519(8)
N6	C31	1.481(7)	C32	C41	1.367(8)
N6	C36	1.350(7)	C33	C35	1.395(8)
N7	C15	1.323(7)	C33	C49	1.396(8)
N7	C51	1.495(7)	C35	C44	1.396(8)
N7	C52	1.366(8)	C36	C37	1.355(8)
N8	C14	1.352(7)	C39	C45	1.406(9)
N8	C38	1.370(7)	C42	C43	1.387(9)
N8	C40	1.486(7)	C43	C46	1.382(10)
C1	C2	1.509(6)	C45	C46	1.396(9)
C1	C3	1.425(7)	C46	C51	1.547(8)
C1	C8	1.362(7)	C48	C49	1.378(8)
C3	C4	1.426(6)	C50	C52	1.377(9)
C3	C12	1.430(7)			

[1]+X,+Y,-1+Z;[2]1+X,1+Y,+Z

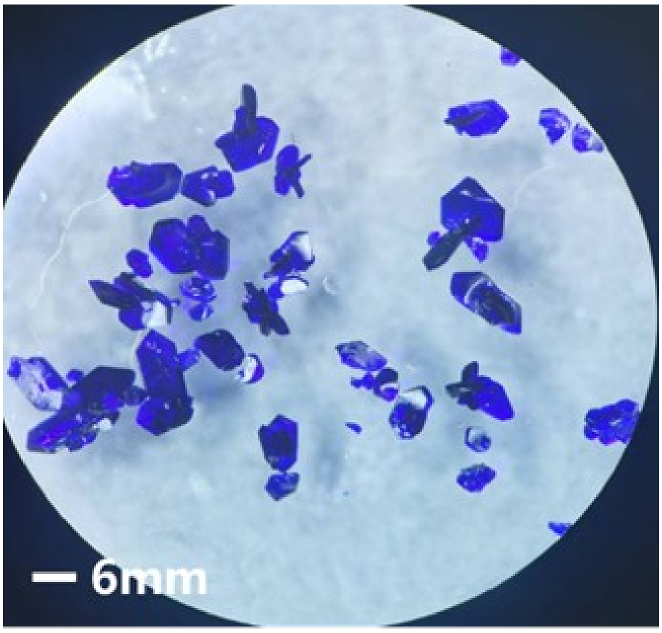

Fig S1. The morphology of JLNU-15.

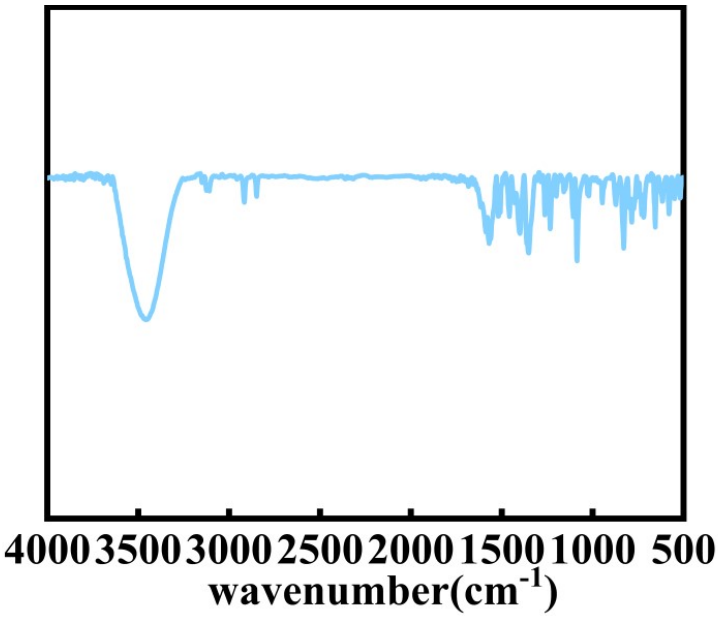

Fig S2. The FT-IR of JLNU-15.

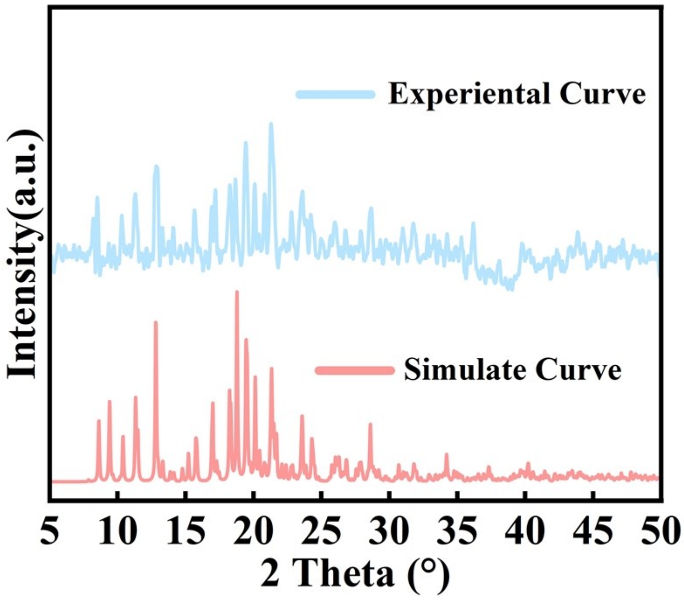

Fig S3. The PXRD pattern of JLNU-15.

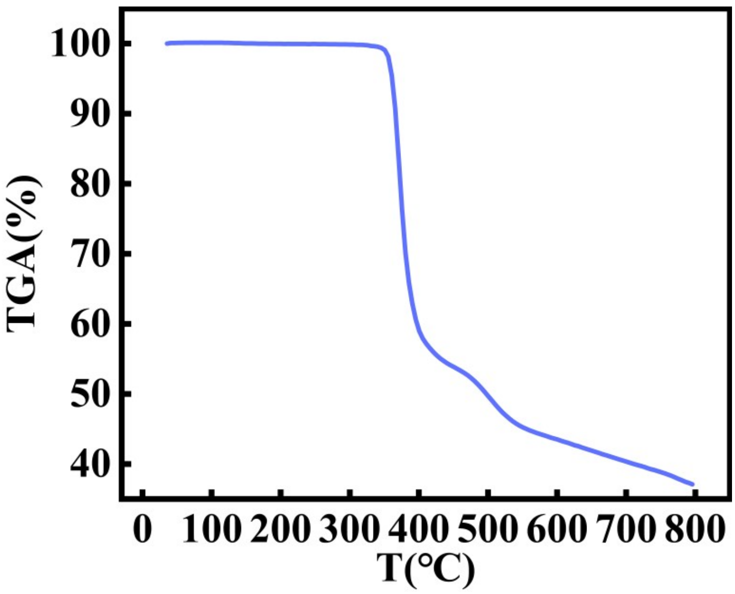

Fig S4. The TGA pattern of JLNU-15.

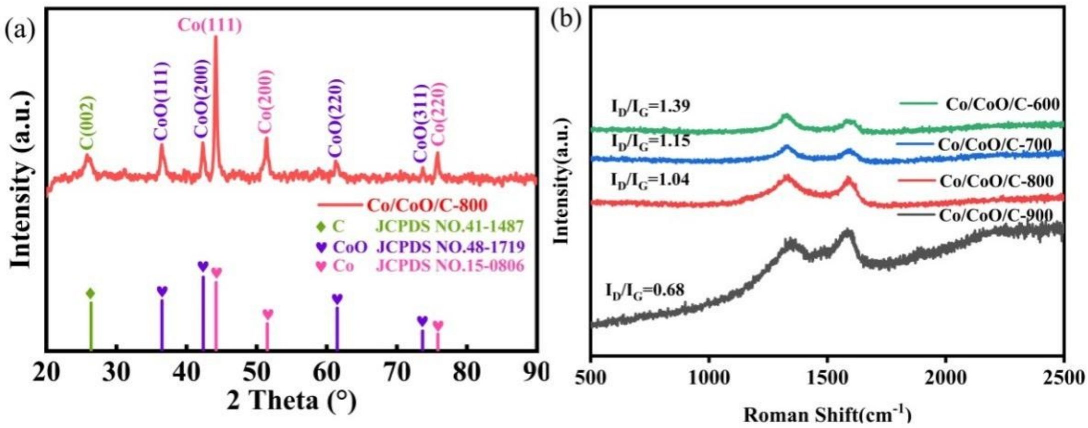

Fig S5. (a) PXRD pattern of Co/CoO/C-800. (b) Raman spectroscopy of Co/CoO/C-600, Co/CoO/C-600-700, Co/CoO/C-600-800 and Co/CoO/C-600-900.

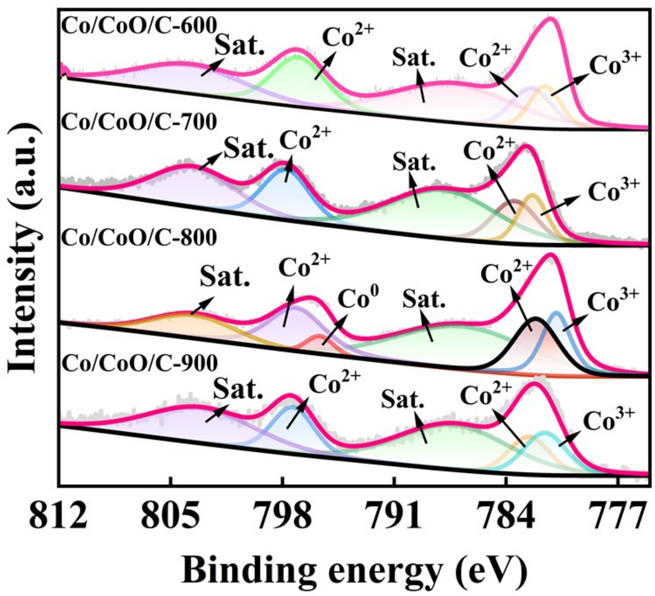

Fig S6. Co 2p XPS spectrum of Co/CoO/C-T (T= 600, 700, 800, 900).

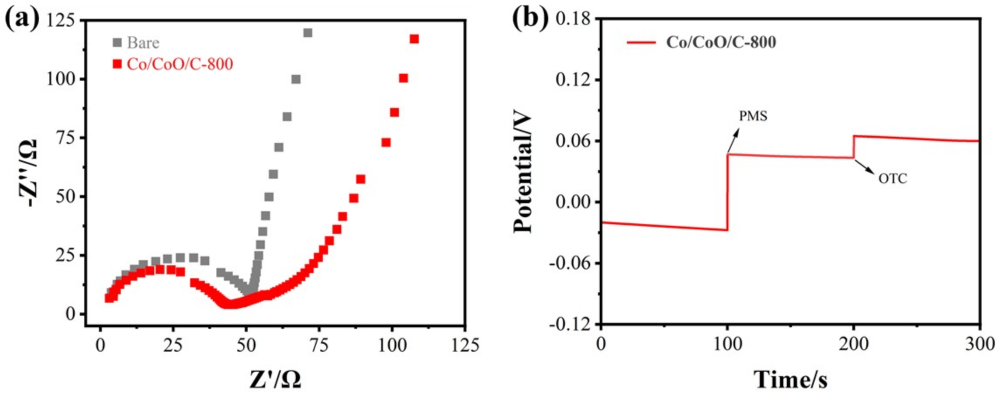

Fig. S7 (a) Electrochemical impedance spectroscopy tests of the without any active material and the Co/CoO/C-800 composite; (b) open-circuit potential test of adding PMS and pollutants.

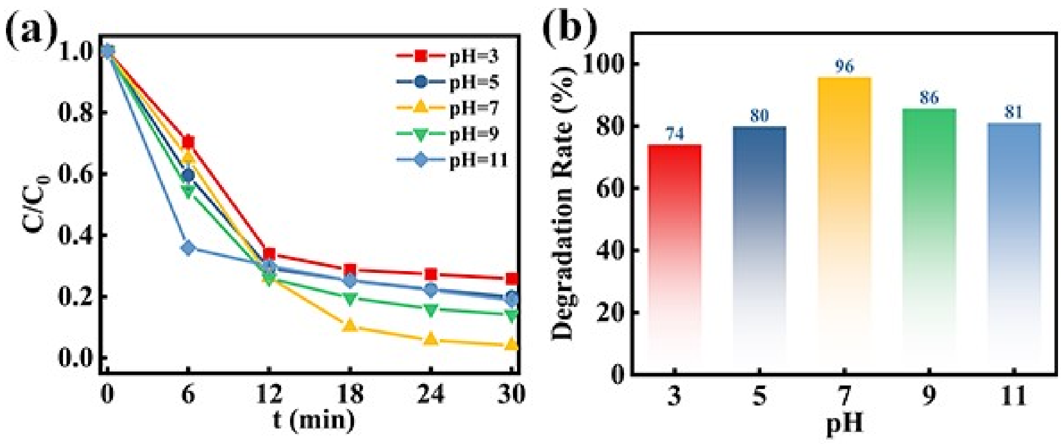

Fig S8. (a) pH-dependent variations in OTC decomposition effectiveness. (b) The degradation rate of Co/CoO@C-800/PMS system over a wide pH range. [Catalyst amount = 0.12 g/L, PMS amount = 0.24 g/L, Pollutant Concentration = 20 mg/L], pH = 3-11, T=298K.

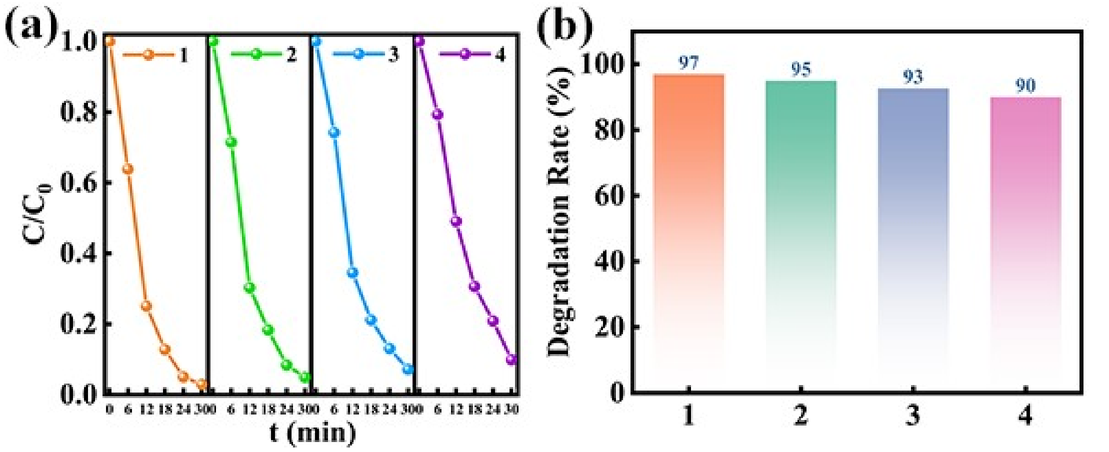

Fig S9. (a) The reusability tests of Co/CoO/C-800 degradation of OTC. (b) The degradation efficiency of every cycle.[Catalyst amount = 0.12 g/L, PMS amount = 0.24 g/L, Pollutant Concentration = 20 mg/L], pH = 7.0, T=298K.

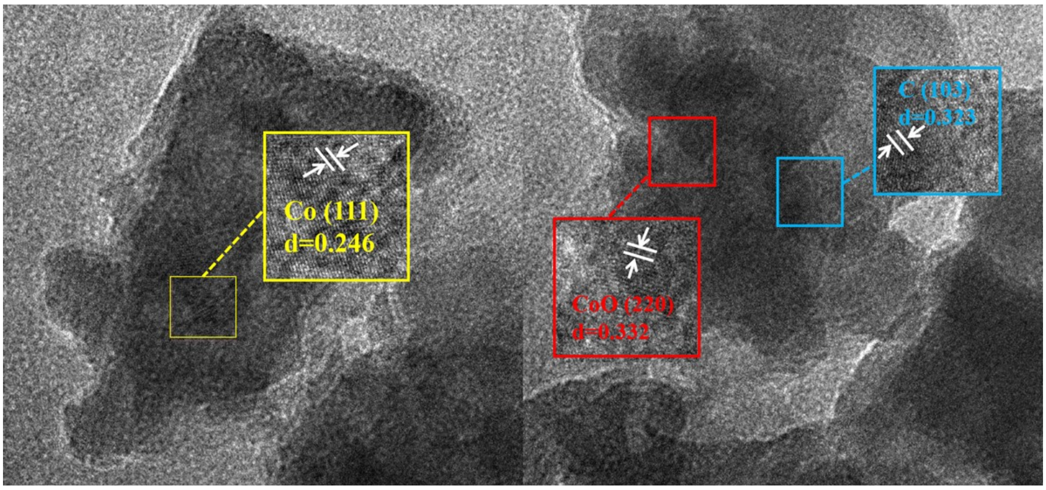

Fig. S10 TEM image after cycling